Effect of Charge on Aerodynamic Breakup of Charged Water Droplet

Yuan-Ping Huo, Jun-Feng Wang*, Zi-Wen Zuo, Zhen-Tao Wang

School of Energy and Power Engineering, Jiangsu University, 212013, Zhenjiang, China
*(*Email: wangjunfeng@ujs.edu.cn)*

Abstract. This study concerns experimentally the secondary breakup morphology of water charged droplets with the action of aerodynamic force in the dripping mode. A new measurement of charge-to-mass ratio has been designed and succeeds in calculating the tiny charge (nC) on a droplet. The high-speed camera combined with a microscopic zoom lens has been used to take images of the breakup morphology of charged and uncharged droplet with air assistance, and the differences which is calculated by the image processing technology is used to analyze the effect of charge on droplet deformation and breakup. The results show that a charged droplet of size 2.8mm is measured to have 50% of the rayleigh charge limit, about 0.51nC. Drop charging enhances drop deformation in the vibrational regime and makes droplet deform more easily because of the lower surface tension caused by electrostatic force. It seems no new breakup modes are observed for charged drop but large differences are observed from breakup morphology and breakup time compared to uncharged drops. And it indicates that charged drop can gain faster breakup equal to uncharged drop of higher We as a result of the electrostatic Weber number.

Keywords: Charged droplet; Air assistance; Secondary Breakup; Charge-to-mass ratio; High-speed camera; Breakup time; Breakup morphology.

1. Introduction

When a droplet carries net electric charge, then the charge resides on the exterior surface due to Coulomb repulsion. If the surface charge density is sufficiently high, the interface becomes unstable, and the droplet disrupts. This phenomenon of Charged secondary breakup was firstly discovered by Bose [1] in 1745 and was theoretically studied by Lord Rayleigh as early as 1882[2]. Then the pioneering works for systematic experimental studies were reported by Zeleny in 1917 [3] and the insightful theoretical electrodynamic models were presented by Taylor in 1964/1966 [4]. There are obvious advantages for electrostatic atomization such as ultra fine droplets, disperse uniformly, easily Controlled, equal deposition and more absorption, so widely applications has been taken in pesticide spraying, industrial coating, mass spectrometry, biotechnology and made new progress in renewable energy technology such as electrostatic spray combustion, preparation of thin film solar cell, liquid-liquid electrostatic spray etc. Investigation on charged droplet deformation and breakup which plays an important role in electro hydrodynamics is the key to reveal the electrostatic atomization mechanisms, however, the effects of electric force and aerodynamic force on drop breakup in industrial application conditions have complex mechanisms, many theoretical and experimental studies are lack of precise explanation, research on this issue has continued from then on. D. R. Guildenbecher and P. E. Sojka [5] (2009) reported an experimental study of the secondary breakup morphology of electrically charged drops. The charge relaxation time and the electrostatic Web number were used to correlate secondary breakup. Raut et al [6] (2009) focused their attention on catastrophic drops breakup in electric field which were suspended in oil, and a new mode of drop breakup in electric fields was

discovered. Gomez and Tang[7] (1993) concerned experimentally the charge and size of droplets generated in electrostatic sprays. Plich and Erdman[8] (1987) compiled early research results and proposed a breakup regime map based on the Weber (We) and Ohnesorge (Oh) numbers. However, there are very few reported experiments on charged droplet air-assisted breakup, so remedying this situation is the major goal of this paper.

2. Experimental Set-up and Methods

2.1 Charged Droplet Air-assisted Breakup Systems

Charged droplet air-assisted breakup experimental device has been designed to study the charged droplet breakup morphology with different air velocities. As shown in Fig.1, The syringe pump (ATI Orion M361) is used to precisely control the flow rate , about 0.075ml/min. Contact charging is used to make drop charged by the high voltage supply with its negative connected to the capillary. Air blower provides different air velocities in order to gain different breakup regimes. Depending on the high-speed camera (MotionPro^{TM}X4puls) and a microscopic zoom lens (NAVITAR12X), the breakup morphology of the charged and uncharged droplets with air assistance is captured. LED cold light source is placed closely ahead of high speed camera and rightly faces the breakup area so that clearer images can be captured in a very short exposure time. In order to ensure the accuracy and safety some key experimental components need to be insulated and the experimental measurement equipments should be grounded.

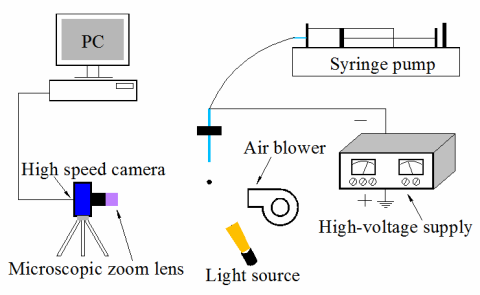

Fig.1. Charged droplet air-assisted breakup experimental device

2.2 Measurement of Charge-to-Mass Ratio for Charged Droplets

Fig.2 shows the home-made device for measuring the charge on a droplet, which consists of two copper plates with their distance 35mm and -7kV applied between them. Then a uniform electric field with its electric intensity $E = 2\times10^5 V/m$ is formed. The Teflon plates are used to make sure the two copper plates insulated with each other. The device designed here has successfully gained the tiny charge (nC) on a charged droplet.

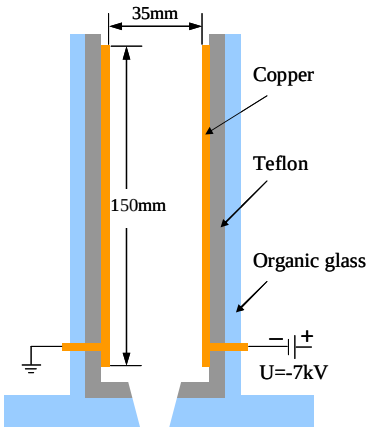

Fig.2. Measurement device

The measuring principle of the device is shown in fig.3. When a charged drop perpendicularly enters the uniform electric field caused by two plate copper electrodes, the drop will do uniformly accelerated motion in the horizontal direction due to the uniform electric field. With the help of high-speed camera (MotionPro^{TM}X4puls), the drop path will be recorded as a series of images. Then three pictures with the same time interval Δt are chosen, and the image processing technology is used to measure the motion distance S_1 and S_2 in the horizontal direction. According to the principle of uniformly accelerated motion:

$$S_1 = v_0\Delta t + \frac{1}{2}a\Delta t^2 \quad (1)$$

$$S_2 = v_1\Delta t + \frac{1}{2}a\Delta t^2 \quad (2)$$

$$v_1 = v_0 + a\Delta t \tag{3}$$

The horizontal acceleration a can be calculated by uniting Eq. (1), (2) and (3):

$$a = \frac{S_2 - S_1}{\Delta t^2} \tag{4}$$

From the uniform electric field, the horizontal acceleration a also can be written as:

$$a = \frac{Uq}{md} \tag{5}$$

Making Eq. (4) equal to (5) and the charge-to-mass ratio for a charged drop will be given as:

$$\frac{q}{m} = \frac{d(S_2 - S_1)}{U\Delta t^2} \tag{6}$$

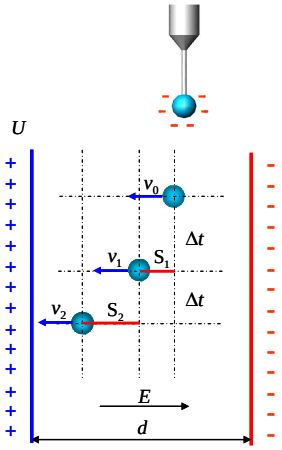

Fig.3. Schematic of measurement of charge-to-mass ratio for charged droplet

3. Results and Discussion

Experiment mainly studies the effect of charge on droplets air-assisted breakup morphology. The capillary No.16 (inner diameter 1.37mm, external diameter 1.6mm) and No.9 (inner diameter 0.67mm, external diameter 0.9mm) are used to produce charged droplets with whose sizes equal to an uncharged droplet produced by the capillary No.7 (inner diameter 0.27mm, external diameter 0.5mm). The home-made measuring device is used to measure the charge-to mass ratio of charged droplets.

3.1 Mechanism of Drop Formation

For uncharged drop, a drop is formed as a result of the imbalance of the adsorption condition that gravity exceeds adsorption force; the size of the spherical drop is given by [9]:

$$\mathrm{D} = \left(\frac{6d_0\sigma_0}{\rho g}\right)^{1/3} \tag{7}$$

Here σ_0 is the surface tension and ε is the permittivity of free space. For a water droplet that dripping freely from the capillary No.7, Eq.(7) will predict its drop size of 2.8mm which is close to the experimental value. However, the surface tension of charged droplet changes greatly and will decrease to [10]

$$\sigma = \sigma_0 - q^2/\left(8\pi^2\varepsilon \mathrm{D}^3\right) \tag{8}$$

Where ε, q, D represents the dielectric constant of the surrounding medium, droplet charge and droplet diameter respectively.

So once droplet is charged, combining Eq. (7) and (8), charged droplet size will theoretically smaller than uncharged one in the same capillary diameter and flow rate. With the help of the high speed camera, Fig.4 shows uncharged and charged drop dripping freely from the same capillary. There are large differences in size dimension between charged and uncharged drops.

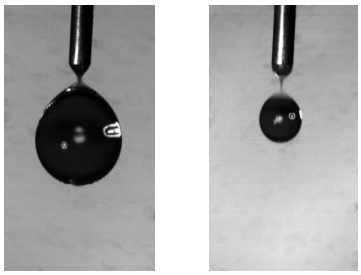

(a) Uncharged (b) Charged

Fig.4. Droplet dripping freely from the capillary

By considering the effect of charge on drop formation process, the capillary No.16 and No.9 are used to produced charged droplets with whose sizes equal to a uncharged droplet (d=2.8mm) produced by the capillary No.7, and the charge on charged drop will be gained with the method in the next paragraph.

3.2 Charge-to-mass Ratio of Charged Droplet

In this part of work, three time intervals (Δt =5ms, 8ms, 10ms) are selected to calculate the charge-to-mass ratio with three groups of pictures for each time interval. For the capillary No.16, Fig.5 shows one group of pictures of charged droplet with the time interval Δt =10ms in a uniform electric field. The motion distance S_1 and S_2 in the horizontal direction are 4.55mm and 5.53mm respectively. According to Eq.(6), the charge-to-mass ratio is calculated to be about $4.89\times10^{-8}C/g$; then other eight groups of pictures are all analyzed with the method above. As shown in Fig.6, an average charge-to-mass ratio $4.48\times10^{-8}C/g$ is gained for the charged droplet with its droplet size 2.8mm. Theoretically, the maximum amount of charge Q_0 a droplet of diameter D may hold is the Rayleigh Limit [11]

$$Q_0 = 2\pi(2\varepsilon\sigma_0)^{0.5}D^{1.5} \qquad (8)$$

Here σ_0 is the surface tension and ε is the permittivity of free space. And the maximum charge-to-mass ratio H_0 is given by:

$$H_0 = \frac{Q_0}{m} = 12(2\varepsilon\sigma_0)^{0.5}\rho^{-1}D^{-1.5} \qquad (8)$$

At this point the H_0 for a charged drop of size 2.8mm is about $9.23\times10^{-8}C/g$; therefore the tiny charge of the charged droplet used in the experiment has about 50% of the Rayleigh charge limit. With the same method above, for charged droplet of size 2.8mm produced by capillary No.9, the average charge-to-mass ratio $2.87\times10^{-8}C/g$ is obtained and has about 32% of the Rayleigh charge limit.

3.3 Charged Droplet air-assisted breakup

For uncharged air-assisted breakup droplets, deformation and breakup mainly depends on the aerodynamic （ $0.5\rho_g u_d^2 D$ ） and the ratio （ σ/D ）of surface tension to droplet diameter, it can be described by a crucial dimensionless number of atomization theory called Weber number [12]

$$We = \frac{\rho_g u_d^2 D}{\sigma} \qquad (9)$$

Where ρ_g and u_d represent gas density and the initial relative velocity between liquid drop and ambient respectively. But to charged

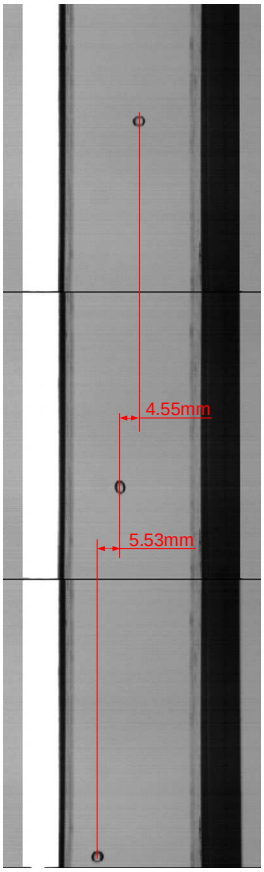

Fig.5. Position of charged droplet with the time interval Δt in a uniform electric field

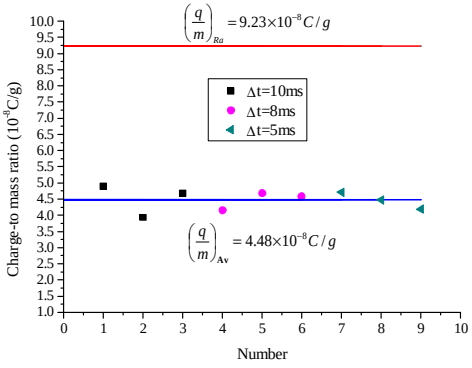

Fig.6 Charge-to-mass ratio with the time interval Δt in a uniform electric field

droplet, drop charging affects droplet deformation, the Eq. (9) are revised using an electrostatic Weber number, We^* [5],

$$We^* = \frac{\rho_g u_d^2 D}{\sigma - q^2/8\pi^2\varepsilon_0 D^3} = \frac{We}{1 - q^2/8\pi^2\varepsilon_0\sigma D^3} \quad (10)$$

Fig.7 (a) shows uncharged drop vibrational morphology ($We \approx 7$) with drop size 2.8mm and the initial relative velocity 13.6m/s. At this regime the drop vibrates constantly, which has the axial maximum diameter 4.19mm and the radial maximum diameter 3.45mm. With the same drop size and initial relative velocity, the charged drop vibrational morphology is given in Fig.7 (b). The charge distributed at the drop surface is about 0.51nC which has 50% of the rayleigh charge limit, but it seems that charged drop still maintain vibrational regime and no new breakup modes are observed. However, drop charging enhances drop deformation in the vibrational regime with the axial maximum diameter 4.93mm and the radial maximum diameter 4.61mm which are all larger than uncharged ones. It indicates charged droplets deform more easily because of the lower surface tension caused by electrostatic force.

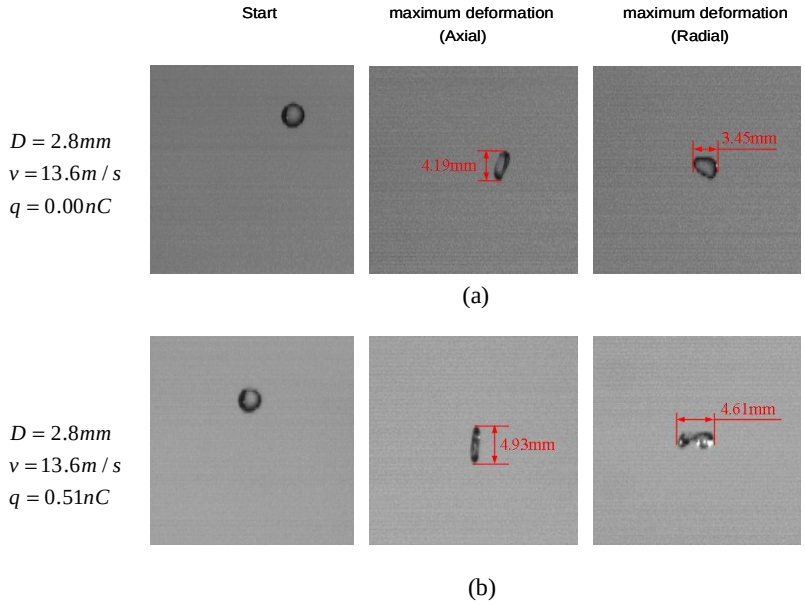

Fig.7. Uncharged (a) and charged (b) water drop vibrational morphology

Traditional secondary atomization modes of an uncharged droplet include bag breakup mode, multimode, stretching-thinning mode and catastrophic breakup mode, and among them bag breakup morphology includes four states: deformation, bag growth, bag breakup and ring breakup. So the bag breakup was achieved when the ring began to breakup and this can be obtained by analyzing the pictures captured by the high-speed camera. In this section, we aim to examine the effect of charge on droplet bag breakup state. As shown in Fig.8 (a)-(d), Bag breakup morphology for uncharged and different charged water droplets is observed. From Fig.8 (b) and (c), it seems that no new breakup modes are obtained for charged droplets which have 32% and 50% of the Rayleigh charge limit respectively. However, large differences are observed from the parts of breakup morphology and breakup time for droplets with different charge. Fig.8 (a) shows about 1.7ms is needed for uncharged droplet with whose size 2.8mm and the initial relative velocity 13.6m/s to achieve bag breakup state. Compared to uncharged drops, there only needs about 1.2ms for charged drop (0.33nC) to achieve this process which can be obviously observed in Fig.8 (b). And bag elongation before breakup is

shorter than uncharged ones in the same experimental situation. Fig.8 (c) shows just 1ms is needed for charged drop with its charge 0.51nC to achieve bag breakup state and bag elongation before breakup is the shortest compared to (a) and (b). This may illustrate breakup will be enhanced as the charge on a droplet increases. Breakup morphology for uncharged drop, of size 2.88mm and the initial relative velocity 20.5m/s, is given in Fig.8 (d).

Compared to Fig.8 (c), the breakup time and bag elongation of uncharged droplet are basically the same as charged droplet (0.51nC) at low air velocity 17.2m/s. It indicates that charged drop at low air velocity can gain quick breakup equal to uncharged drop of higher air velocity as a result of the electrostatic Weber number We^* referred to Eq.(12) which applies to charged droplet with the action of aerodynamic force.

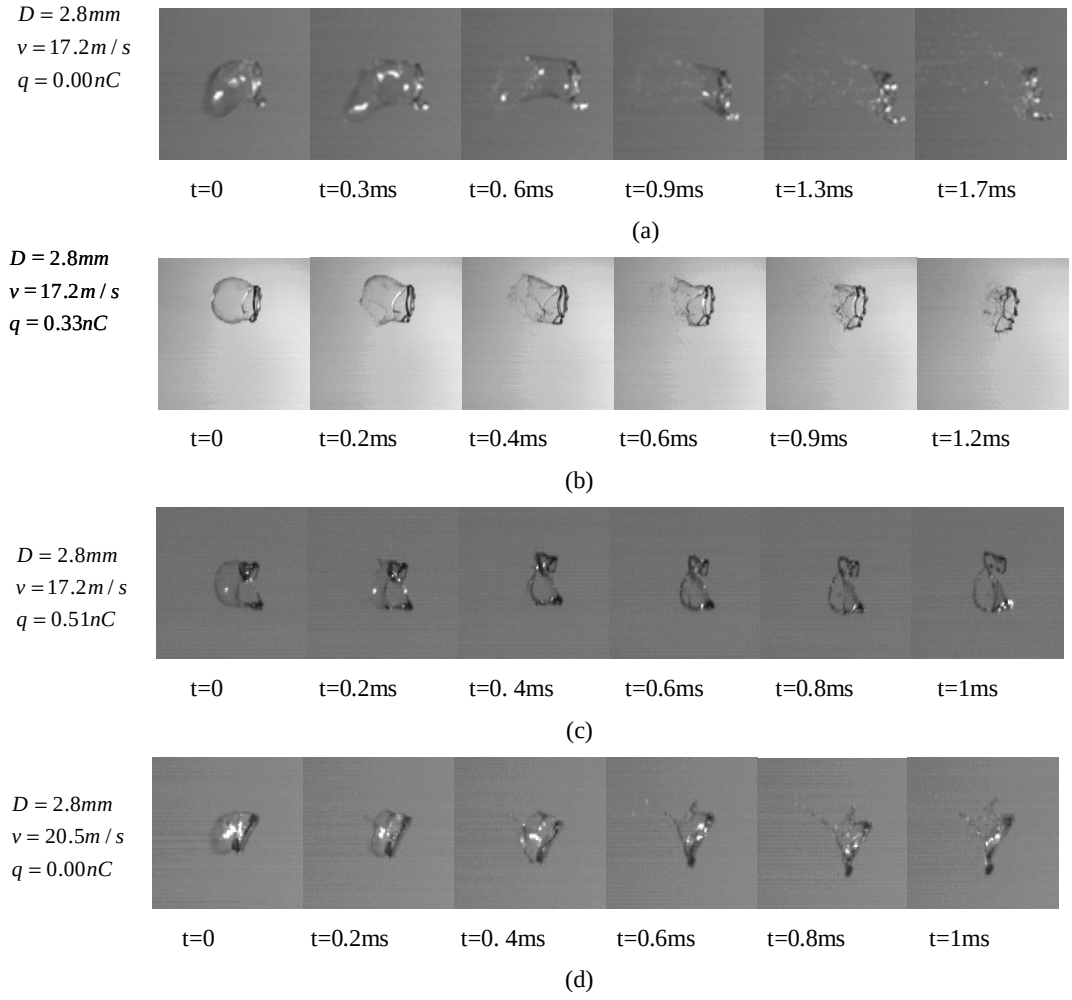

Fig.8. Uncharged (a), (d) and charged (b), (c) drop bag breakup morphology

4. Conclusion

An experimental investigation was conducted to study droplet air-assisted deformation and breakup morphology with a given charge. A homemade measurement device has successfully gained the tiny charge of a droplet of size 2.8mm, about 0.51nC for capillary No.16 which is 50% of the Rayleigh charge limit and 0.33nC for capillary No.9 which is 32% of the Rayleigh charge limit. Drop charging enhances drop deformation in the vibrational regime and makes droplet deform more easily because of the low

surface tension caused by electrostatic force. There are no new breakup modes been observed for charged drop in the bag breakup regime but large differences are observed from breakup morphology and breakup time for droplet with different charge. Higher charge means less breakup time and shorter bag elongation As a result of the electrostatic Weber number We^*, charged drop can gain faster breakup equal to uncharged drop of higher air velocity.

However, a comprehensive understanding of charged drop air-assisted breakup has heretofore been lacking. Future investigation will firmly focus on drop air-assisted breakup morphology of other regimes include multimode, stretching-thinning and catastrophic breakup modes. The behavior of charged droplet breakup needs to be completed in the future work.

5. Acknowledgments

This research is supported by NSFC 51006047 and 51106064, the authors appreciate their support.

6. References

1. Bose G M. Philos. Trans. R. Soc. London, 1748, 45, 187.

2. Rayleigh, Lord *phil. Mag*, 1882, 14, 184-186.

3. Zeleny, J. *Phys. Rev*, 1917, 10, 1-6.

4. Taylor, G. *Proc. R .Soc.* London, 1964, A280, 383-397.

5. Guildenbecher, C. *IMECE2007*.Washington. 2007.

6. Raut J S,C. Langmuir. 2009. 25(9), 4829-4834.

7. Gomez and Tang, J. *Phys. Fluids*, 1994, 6, 1.

8. Plich, M, and Erdman, C. A, *International Journal of Multiphase Flow*, 1987, 13(6), 741-757.

9. Eow J S, Ghadiri M，Sharif A. J, *Journal of Electrostatics*.2001, (51-52), 463-469.

10. Junfeng Wang. Investigation on electrospray of fuel and charged two phase turbulent jet flow, D. Zhenjiang: Jiangsu University, 2002.

11. Shrimpton, J, S. J. *IEEE Transactions on Dielectrics and Electrical Insulation*, 2005, 12(3), 573-575

12. Weber, C. Disintegration of liquid jets, Z. *Angew. Math. Mech.*, 1931, 11 (2), 136-159